Structures and Stereodynamics of *N*-9-Triptycylacetamide and Its *N*-Alkyl Derivatives

Gaku Yamamoto,* Fusako Nakajo, Natsuko Tsubai, Hiroaki Murakami, and Yasuhiro Mazaki

Department of Chemistry, School of Science, Kitasato University, Kitasato, Sagamihara, Kanagawa 228-8555

(Received April 7, 1999)

X-Ray crystallographic and dynamic NMR spectroscopic studies were performed on *N*-9-triptycylacetamide (**1**), *N*-methyl-*N*-9-triptycylacetamide (**2**), *N*-ethyl-*N*-9-triptycylacetamide (**3**), and *N*-benzyl-*N*-9-triptycylacetamide (**4**). In the crystalline state, compounds **1**, **2**, and **4** exist solely as the *Z*-isomer for the amide bond, while equal amounts of the *Z*- and *E*-isomers exist in a single crystal of compound **3**. The amide nitrogen atom in **2**, **3**, or **4** is significantly pyramidalized. In solution, **1** exists solely as the *Z*-isomer, while **2**, **3**, and **4** exist as an equilibrium mixture of the *Z*- and *E*-isomers. The isomer ratio is not correlated with the bulkiness of the *N*-alkyl group; the *N*-ethyl compound **3** seems to behave anomalously. The isomer ratio is significantly dependent on the solvent; the population of the *Z*-isomer in **2** or **3** or **4** increases with the solvent polarity. The $Z \rightleftarrows E$ interconversion takes place on the NMR time scale around ambient temperature, and the barrier is dependent on the solvent; hydroxylic solvents, methanol and ethanol, increase the barrier. The methylene protons in the ethyl or benzyl group in any isomer of **3** or **4** become diastereotopic at low temperatures suggesting that the nitrogen atom in either compound is pyramidal in solution. Stereomutation around the Tp–N bond is discussed in some detail.

Static and dynamic stereochemistry of amide bonds has long been extensively studied.[1] The amide moiety is usually characterized by a planar geometry with the trigonal-planar nitrogen and carbonyl carbon atoms, and a high energy barrier to rotation about the N–C(O) bond because of the conjugation between the nitrogen atom and the carbonyl group, although some recent theoretical investigations doubt this notion.[2] Although the amide moiety is planar in most acyclic amides, distortion of the amide moiety has attracted much attention.[3] Twisting of the N–C(O) bond and concomitant pyramidalization of the nitrogen atom have been observed in bridgehead lactams,[3] and in amides where the nitrogen is incorporated in a ring system.[4,5]

We have been interested in dynamic stereochemistry of various derivatives of 9-triptycylamine; *N,N*-dialkyl-9-triptycylamines,[6] *N*-phenyl-9-triptycylamine derivatives,[7] and *O*-phenyl-*N*-9-triptycylhydroxylamine.[8] In this article, we report our recent studies on molecular structures in the crystalline state and dynamic stereochemistry in solution of *N*-9-triptycylacetamide (**1**) and its derivatives **2**—**4** with a primary alkyl group attached to the nitrogen atom (Chart 1).[9] The principal interest is how the bulky 9-triptycyl (Tp) group will affect the molecular geometry, the *E*/*Z* isomeric equilibrium of the amide moiety, and the rotational barrier of the amide bond. Furthermore, stereodynamics of the Tp–N bond is another subject of special interest.

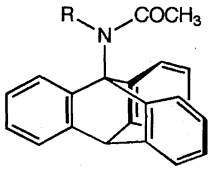

1: R=H
2: R=CH_3
3: R=C_2H_5
4: R=$CH_2C_6H_5$

Chart 1.

Results and Discussion

Syntheses. *N*-9-Triptycylacetamide (**1**) and its *N*-alkyl derivatives **2**—**4** were synthesized as outlined in Scheme 1; 9-triptycylamine (**5**) was first converted to its *N*-alkyl derivatives and then *N*-acetylated. *N*-Methyl-9-triptycylamine (**6**) was prepared by direct methylation of **5** with methyl iodide instead of dimethyl sulfate used in the previous report.[6b] *N*-Ethyl-9-triptycylamine (**7**) was obtained by reduction of compound **1** with BH_3·THF in place of the direct alkylation of compound **5** previously reported.[6b] *N*-Benzyl-9-triptycylamine (**8**) was prepared by reduction with BH_3·THF of *N*-9-triptycylbenzamide (**9**) obtained by reaction of **5** with benzoyl chloride. Use of $LiAlH_4$ as the reducing agent gave poorer results as compared with BH_3·THF; compound **1** gave **7** in 36% yield but **9** did not afford **8** in detectable amounts.

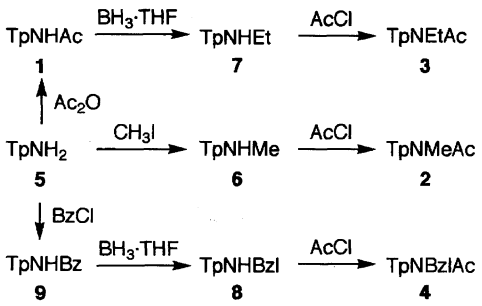

Scheme 1.

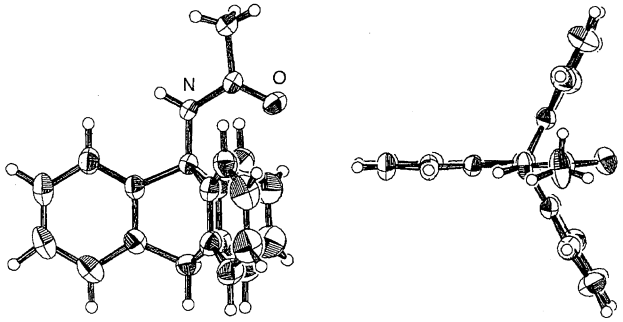

Fig. 1. Side and top views of the molecular structure of compound **1**.

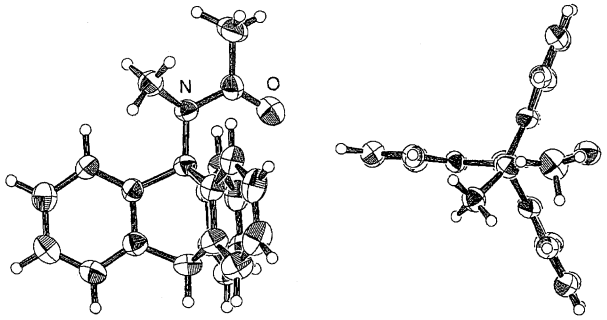

Fig. 2. Side and top views of the molecular structure of compound **2**.

N-Acetylation of **5** and its *N*-alkyl derivatives **6**—**8** was made with the use of either acetic anhydride or acetyl chloride. For compounds **5**—**7**, where steric hindrance is rather small, either reagent gave satisfactory results, but compound **8** could not be acetylated with acetic anhydride.

X-Ray Crystallographic Analysis. In order to examine the molecular structures of **1**—**4** in the crystalline state, X-ray crystallographic analysis was performed for single crystals of these compounds. Perspective drawings of the molecular structures for **1**—**4** are shown in Figs. 1, 2, 3, and 4 though those for **1**—**3** have already been given in the preliminary reports.[9] Selected bond lengths, bond angles, and torsional angles for **1**—**4** are compiled in Table 1 with the numbering shown in Scheme 2.

Compound **1** exists in a near C_s geometry with the acetyl group bisecting two *o*-benzeno groups of the Tp moiety, and the amide bond adopts *Z* configuration (Fig. 1). The nitrogen atom is assumed to be planar, though the position of the N–H hydrogen is not precisely determined.

In compound **2**, two independent molecules, **A** and **B**, are present in a crystal, both of which are in *Z* configuration. As

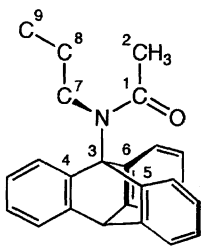

Scheme 2.

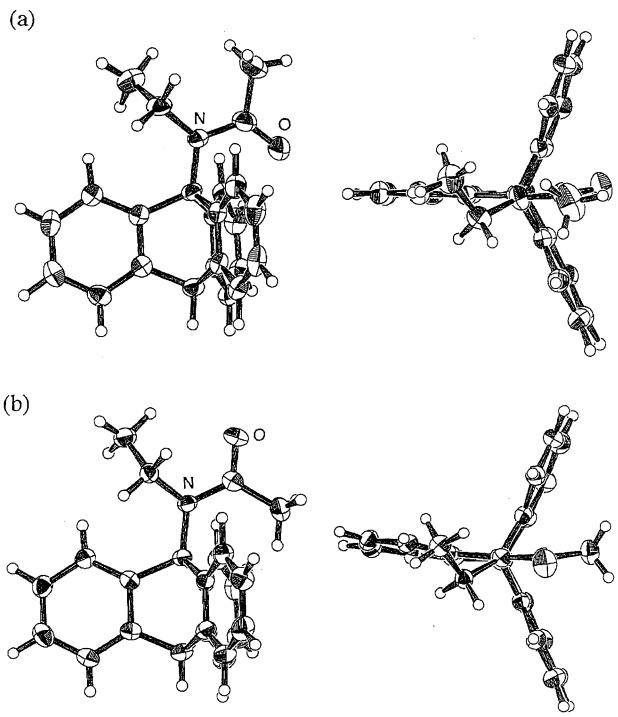

Fig. 3. Side and top views of the molecular structures of (a) (*Z*)-**3** and (b) (*E*)-**3**.

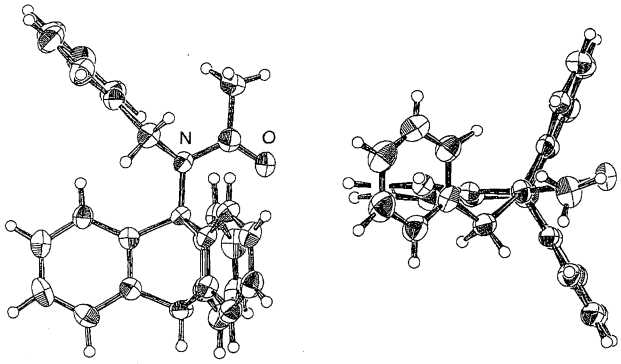

Fig. 4. Side and top views of the molecular structure of compound **4**.

no significant difference in geometry are observed between the two molecules, only molecule **A** is shown in Fig. 2. In either molecule the amide nitrogen atom is significantly pyramidalized, and the sum of the three bond angles around the nitrogen is 352°, considerably smaller than 360° expected for the planar geometry.

For compound **3** recrystallized from ethanol, two independent molecules are present in a crystal again, but in this case one is in *Z* and the other in *E* configuration (Fig. 3). Crystals recrystallized from toluene have the same crystal structure as those from ethanol, and thus this situation seems independent of the crystallization solvent. Co-existence of two or more rotational isomers in a single crystal seems a rather rare phenomenon, although not unprecedented.[10] The nitrogen atom is also pyramidalized in either isomer. The sum of the three bond angles around the nitrogen is 357.0° and 354.4° for (*Z*)-**3** and (*E*)-**3**, respectively, and thus the

Table 1. Selected Bond Lengths, Bond Angles, and Torsional Angles around the Amide Moietey[a)]

Compd	1	2		3		4
		A	B	*Z*	*E*	
C1–O	1.230(2)	1.225(3)	1.219(3)	1.218(2)	1.227(2)	1.214(4)
C1–N	1.352(2)	1.379(3)	1.382(3)	1.378(2)	1.383(2)	1.396(4)
C1–C2	1.495(2)	1.508(4)	1.513(4)	1.521(3)	1.506(3)	1.504(5)
N–C3	1.450(2)	1.472(3)	1.465(3)	1.477(2)	1.474(2)	1.481(4)
N–C7		1.482(3)	1.495(3)	1.479(2)	1.487(2)	1.495(4)
C1–N–C3	122.7(1)	117.6(2)	119.0(2)	116.1(1)	121.3(1)	117.0(2)
C1–N–C7		116.7(2)	115.8(2)	119.7(1)	112.7(1)	115.6(3)
C3–N–C7		117.7(2)	117.1(2)	121.2(1)	120.4(1)	117.3(3)
Sum		352.0	351.9	357.0	354.4	349.9
O–C1–N	122.1(1)	122.5(2)	123.1(2)	122.6(2)	119.8(3)	121.9(3)
O–C1–C2	121.7(2)	120.8(2)	120.7(2)	119.1(2)	117.9(4)	120.8(4)
N–C1–C2	116.3(2)	116.7(2)	116.2(2)	118.4(1)	122.3(3)	117.3(3)
Sum	360.1	360.0	360.0	360.1	360.0	360.0
N–C3–C4	114.0(1)	115.9(2)	114.3(2)	120.4(1)	118.3(1)	116.2(2)
N–C3–C5	113.3(1)	114.3(2)	116.1(2)	110.0(1)	111.2(1)	111.6(3)
N–C3–C6	113.9(1)	111.7(2)	111.8(2)	112.0(1)	113.4(1)	114.4(3)
C3–N–C1–C2	−177.7(2)	179.7(2)	178.7(3)	−174.2(2)	7.1(2)	−173.6(4)
C3–N–C1–O	2.5(3)	2.3(3)	0.6(3)	6.1(3)	−171.2(2)	8.3(5)
C7–N–C1–C2		−32.2(3)	−33.5(4)	−13.5(3)	160.7(2)	−28.9(5)
C7–N–C1–O		150.4(2)	148.4(2)	166.8(2)	−17.6(2)	152.9(3)
C1–N–C3–C4	180.0(2)	−170.3(2)	−165.9(2)	−176.9(2)	−175.5(2)	−173.7(3)
C1–N–C3–C5	61.6(2)	69.2(2)	73.0(3)	62.9(2)	62.7(2)	65.1(4)
C1–N–C3–C6	−61.2(2)	−54.2(2)	−50.0(2)	−58.5(2)	−60.3(2)	−57.5(4)
C7–N–C3–C4		42.0(2)	46.7(3)	22.7(2)	32.9(2)	42.2(4)
C7–N–C3–C5		−78.6(2)	−74.4(2)	−97.5(2)	−88.9(2)	−79.0(4)
C7–N–C3–C6		158.1(2)	162.6(3)	141.1(2)	148.1(1)	158.4(3)
C3–N–C7–C8				−105.6(2)	−120.0(2)	−121.6(3)
N–C7–C8–C9						−176.4(3)

a) Bond lengths are given in Å, and angles in °. See Scheme 2 for the numbering.

degree of pyramidalization is somewhat smaller than in **2**.

Compound **4** exists solely in *Z*-configuration in the crystalline state (Fig. 4). Pyramidalization of the nitrogen is the largest among the compounds examined in this study, the angle sum at nitrogen being 349.9°.

Noteworthy in the *N*-alkyl derivatives **2**—**4** is that the acetyl group nearly bisects the two *o*-benzeno groups; the carbonyl carbon is planar and the plane of the acetyl group is almost coplanar with the plane made of N, C3, and C4. Meanwhile the α-carbon of the *N*-alkyl group is significantly out of the plane made of N, C3, and C4, the torsional angle C7–N–C3–C4 ranging between 23° and 47°. This suggests that the pyramidalization may be due to steric effects. The *N*-alkyl group should eclipse the third *o*-benzeno group if the nitrogen were planar, and in order to avoid this situation the nitrogen should pyramidalize.

Bond lengths around the amide moiety depend on the group R. As R becomes bulkier, the C–N bond elongates ($\mathbf{1} < \mathbf{2} \approx \mathbf{3} < \mathbf{4}$) and the C=O bond shortens ($\mathbf{1} > \mathbf{2} \approx \mathbf{3} > \mathbf{4}$). Elongation of the C–N bond may be ascribed to the steric repulsion between R and the acetyl-methyl group (or the carbonyl oxygen in case of (*E*)-**3**), and this may decrease the contribution of the polarized resonance structure, which will in turn result in the shortening of the C=O bond.

***E/Z* Isomerism in Solution.** The ^{1}H NMR spectrum of **1** shows a single sharp peak for the acetyl methyl protons in any solvent examined; e.g., at δ = 2.52 in $CDCl_3$ (Table 2). This chemical shift, together with the fact that this signal remains sharp down to −100 °C, suggests that this compound exists in solution solely as the *Z*-isomer for the amide bond. This is further confirmed by the NOE experiment, where irradiation of the acetyl methyl protons results in the enhancement of the NH signal. Therefore compound **1** is concluded to exist as the *Z*-isomer both in crystal and in solution.

For the *N*-alkyl derivatives **2**—**4**, the presence of two isomers, *E* and *Z*, in equilibrium is revealed by NMR in any solvent examined. The lineshape change due to the $Z \rightleftarrows E$ interconversion takes place around room temperature, and extensive thermodynamic and kinetic studies on the isomer equilibria and equilibration were made, which are discussed in this section. At low temperatures, the lineshape change ascribed to stereomutation of the Tp–N bond is observed and will be discussed in a later section.

The isomer assignments are made as follows. In any of

compounds **2**—**4**, two singlet signals ascribable to the acetyl methyl protons are observed, one at $\delta \approx 2.6$ and the other at $\delta \approx 1.6$, in nonaromatic solvents (Table 2). The higher-field signal should be assigned to the *E*-isomer because the acetyl protons in the *E*-isomer are in the shielding region of the ring current effect of the flanking *o*-benzeno groups. The assignment is confirmed by NOE experiments at low temperatures where the $Z \rightleftarrows E$ interconversion is sufficiently slow. For compound **2**, for example, in $CDCl_3$ at -26 °C, where the isomer ratio is ca. 4 : 1, irradiation of the more intense acetyl signal at $\delta = 2.63$ enhances the more intense *N*-methyl signal at $\delta = 3.72$ by ca. 12%, while irradiation of the less intense acetyl signal at $\delta = 1.74$ does not affect the less intense *N*-methyl signal at $\delta = 3.85$, confirming that the former set of signals are assigned to the *Z*-isomer and thus the latter to the *E*-isomer. Similarly, the isomer assignments are unambiguously made for all combinations of compounds and solvents examined.

Table 2 shows that the chemical shifts of the protons around the amide moiety are almost independent of the solvent except for toluene-d_8, an aromatic solvent, though small upfield shifts are generally observed in acetonitrile-d_3. It is noteworthy in Table 2 that, upon changing the solvent from chloroform-*d* to toluene-d_8, significant upfield shifts are observed for the signals assigned to the *Z*-isomer, while no remarkable shifts are observed for the *E*-isomer signals. This feature is consistent with the well-documented tendency in the ASIS (aromatic solvent induced shifts) of amides; an aromatic solvent molecule tends to form a "solvation complex" with an amide so that the carbonyl oxygen is located as far from the π-cloud of the solvent as possible.[11] Such a solvation complex can be more easily formed in the *Z*-isomer than in the *E*-isomer because of steric reasons.

The population ratios of the *Z*/*E* isomers of compounds **2**—**4** at equilibrium were measured by integration of the acetyl proton signals in eight solvents given in Table 3 over the temperature range of ca. 50° except for compound **3** in CCl_4. The van't Hoff plots of the equilibrium constants afforded the thermodynamic parameters given in Table 3. The isomer populations at 300 and 250 K calculated from the data in Table 3 are compiled in Table 4. We assume that the effect of sample concentration on the isomer equilibrium is negligible. For compound **2** in $CDCl_3$ at 23 °C, the equilibrium constant did not depend on the concentration over the range of 5—100 mmol dm^{-3}. All the measurements were made with the sample concentration of less than ca. 100 mmol dm^{-3} (ca.

Table 2. Chemical Shifts (δ) of the Protons Relevant to the Amide Moiety in Various Solvents[a)]

Compd	Proton	CCl_4	$CDCl_3$	CD_2Cl_2	$(CD_3)_2CO$	CD_3CN	CD_3OD	C_2D_5OD	$C_6D_5CD_3$
1	$COCH_3$	b)	2.519	2.508	b)	2.463	2.531	b)	1.939
(*Z*)-**2**	$COCH_3$	2.481	2.605	2.561	2.569	2.471	2.572	2.577	2.029
	NCH_3	3.599	3.704	3.688	3.774	3.599	3.728	3.739	2.914
(*E*)-**2**	$COCH_3$	1.627	1.727	1.658	1.605	1.564	1.650	1.645	1.599
	NCH_3	3.760	3.851	3.801	3.787	3.722	3.822	3.827	3.643
(*Z*)-**3**	$COCH_3$	2.545	2.636	2.578	2.598	2.499	2.596	2.600	2.037
	NCH_2	4.150	4.222	4.195	4.293	4.164	4.303	4.309	3.424
	NCH_2CH_3	1.932	1.925	1.876	1.921	1.812	1.879	1.892	1.282
(*E*)-**3**	$COCH_3$	1.411	1.492	1.426	1.386	1.348	1.414	1.417	1.452
	NCH_2	4.225	4.331	4.276	4.28	4.221	4.331	4.335	4.142
	NCH_2CH_3	1.823	1.839	1.799	1.795	1.760	1.801	1.809	1.811
(*Z*)-**4**	$COCH_3$	2.303	2.387	2.348	2.365	2.280	2.366	2.366	2.003
	NCH_2	5.359	5.419	5.408	5.537	5.420	5.507	c)	4.968
(*E*)-**4**	$COCH_3$	1.651	1.621	1.668	1.628	1.587	1.663	1.659	1.621
	NCH_2	d)	d)	d)	d)	d)	d)	c)	5.312

a) Data were obtained at 23 °C for **1**, at ca. 0 °C for **2** and **4**, and at ca. -15 °C for **3**. b) Not measured. c) Obscured due to the overlap with the solvent OH peak. d) Not detected due to extreme broadening.

Table 3. Thermodynamic Parameters for the $Z \rightleftarrows E$ Equilibrium in Compounds **2**—**4** in Various Solvents[a)]

Solvent	**2**			**3**			**4**		
	ΔH	ΔS	ΔG_{300K}	ΔH	ΔS	ΔG_{300K}	ΔH	ΔS	ΔG_{300K}
CCl_4	1.5±0.1	−0.9±0.4	1.8_0	b)			2.3±0.3	3.4±1.2	1.2_2
$C_6D_5CD_3$	5.2±0.3	7.1±1.0	2.9_7	−0.5±0.1	6.2±0.3	-2.3_4	3.6±0.2	6.4±0.6	1.6_7
$CDCl_3$	6.0±0.5	8.9±1.7	3.3_3	4.0±0.3	18.5±0.8	-1.5_8	4.8±0.4	8.3±1.3	2.2_7
CD_2Cl_2	9.4±0.4	9.4±1.4	6.6_0	7.9±0.1	20.2±0.4	1.8_2	7.2±0.4	9.9±1.5	4.1_7
$(CD_3)_2CO$	10.8±1.3	12.5±5.3	7.0_6	5.6±0.3	13.0±1.2	1.6_7	7.9±0.4	10.7±1.6	4.7_3
CD_3CN	11.3±2.1	8.0±7.7	8.9_2	9.2±0.7	16.1±2.6	4.3_0	7.6±0.9	4.6±3.3	6.2_2
C_2D_5OD	9.4±0.4	14.8±1.5	4.9_4	2.5±0.5	9.0±1.7	-0.1_5	7.4±0.5	12.5±1.6	3.6_1
CD_3OD	9.8±0.4	12.7±1.6	5.9_7	4.1±0.2	9.2±0.8	1.2_9	8.6±0.5	14.0±1.9	4.4_4

a) ΔH and ΔG_{300K} are given in kJ mol^{-1} and ΔS in J mol^{-1} K^{-1}. b) Not measured.

Table 4. Isomer Ratios (*Z*/*E*) in Compounds **2**—**4** at 300 and 250 K[a)]

Solvent	ε[b)]	**2**		**3**		**4**	
		300 K	250 K	300 K	250 K	300 K	250 K
CCl_4	2.24	67/33	70/30		13/87	62/38	66/34
$C_6D_5CD_3$	2.38	78/22	84/16	28/72	27/73	66/34	72/28
$CDCl_3$	4.81	79/21	86/14	34/66	42/58	71/29	78/22
CD_2Cl_2	7.77	93/7	97/3	68/32	80/20	84/16	90/10
$(CD_3)_2CO$	20.7	94/6	98/2	66/34	76/24	87/13	93/7
CD_3CN	37.5	97/3	99/1	85/15	92/8	92/8	96/4
C_2D_5OD	24.6	88/12	94/6	48/52	53/47	81/19	89/11
CD_3OD	32.6	92/8	96/4	63/37	70/30	86/14	92/8

a) Calculated from the data in Table 3 except for **3** in CCl_4, where an observed value at 250 K is cited. b) Dielectric constant of the solvent.

15 mg/0.5 mL solvent).

Substituent effects on the *E*/*Z* equilibrium in amides have generally been explained in terms of steric effects when the substituents are alkyl groups. In *N*-alkyl-*N*-methylacetamides, for example, the population of the *Z*-isomer has been reported to be 51, 53, 55, and 58% for ethyl, butyl, cyclohexyl, and isopropyl, respectively (solvent not specified).[12] The bulkier the alkyl group, the larger the population of the *Z*-isomer. The population of *Z*-**2** is 79% in $CDCl_3$ (Table 4), which is in line with the above tendency.

If the notion of steric crowding is simply applied to the present series of compounds TpNRAc, the population of the *Z*-isomer is expected to decrease with the bulkiness of R: **1** > **2** > **3** > **4**. Experimentally the *Z* population decreases in the order **1** > **2** > **4** > **3** in any given solvent (Table 4). Especially in the *N*-ethyl compound **3**, the *Z* population is below 50% in solvents of low polarity, and this seems quite anomalous according to the above discussion. Preliminary molecular mechanics calculations (MM3) however reproduce the tendency in the experiments. The *Z*-isomer is calculated to be far more stable than *E* in compound **1**. The energy difference between the isomers decreases in the order **1** > **2** > **4** > **3**, and (*Z*)-**3** is less stable than (*E*)-**3** (Table 5). This suggests that not only the simple "bulk" of the substituent such as given by the van der Waals radius but also the consideration of the shape and relative orientation of the substituent is important in predicting the relative stability of conformations.

Table 5. Some Results of the MM3 Calculations

Compd	Isomer	Es[a)]	μ[b)]	Sum[c)]
1	*Z*	0	4.00	356.9
	E	15.2	3.77	359.8
2	*Z*	0	3.75	357.4
	E	6.8	3.82	358.8
3	*Z*	0	3.63	355.1
	E	−1.6	3.84	358.1
4	*Z*	0	3.54	354.0
	E	5.8	3.90	356.2

a) Relative steric energy in kJ mol^{-1}. b) Dipole moment in D. c) Sum of the bond angles around the nitrogen in °.

The calculated geometries generally well reproduce those obtained by X-ray crystallography, though the calculations give considerably shallower pyramids for the nitrogens than those observed (Table 5). It is uncertain whether this should be ascribed to the inadequacy of the force field parameters or to the disregard of the lattice forces in the calculation.

In compounds **2** and **4**, the *Z*-isomer is dominant in any solvent, while in compound **3** the *Z*-isomer is less populated than the *E*-isomer in solvents of low polarity such as CCl_4, toluene, and chloroform. The population of the *Z*-isomer tends to increase with the polarity of the solvent, though the behavior in the hydroxylic solvents is not straightforward (Table 4). This seems to suggest that the *Z*-isomer has a larger dipole moment than the *E*-isomer. The MM3 calculations however predict a larger dipole moment for the *E*-isomer, although the difference between the isomers is very small (Table 5). The lone-pair electrons on the amide nitrogen might be inadequately considered in the calculations, especially when the nitrogen is significantly pyramidalized as in the present cases. Anyway the results of the MM3 calculations should be cautiously treated.

In hydroxylic solvents, CD_3OD and C_2D_5OD, the population of the *Z*-isomer is lower than that in acetone with a smaller ε value for any of **2**—**4**. Considerations of molecular models show that the carbonyl oxygen of the *E*-isomer seems sterically more exposed to the approach of solvent molecules than that of the *Z*-isomer and thus the stabilization due to hydrogen bonding by solvent molecules would be larger in the *E*-isomer than the *Z*-isomer. This effect may partially cancel the polarity effect resulting in the observed population ratios.

***E*⇄*Z* Isomerization.** Kinetic studies of the *E*⇄*Z* interconversion in compounds **2**—**4** were made using total lineshape analysis (TLA) and saturation transfer (ST) experiments. TLA was made for the acetyl methyl, *N*-methyl, and the bridgehead proton (10-H) signals for each compound, and the most consistent rate constant was determined for each temperature. In ST experiments, the change in the intensity of the acetyl methyl signal of the *Z*-isomer was measured upon irradiation of the corresponding signal of the *E*-isomer. Nonlinear least-squares analysis of the obtained data afforded the rate constant for the *Z*→*E* process. Least-

squares analysis of the Eyring plot of the rate constants thus obtained gave the kinetic parameters, which are compiled in Table 6.

Energy barriers to rotation of the amide bond are mainly electronic in origin; the amide resonance at the ground state is lost at the transition state for rotation.[1] If only the steric effect of substituents is important, the barrier would be lowered as the bulkiness of the substituent attached to the amide moiety increases, because the ground state is more crowded than the transition state for rotation. For example, in a series of *N*,*N*-dimethylamides $RCON(CH_3)_2$, $\Delta G^{\ddagger}$ are 87, 76, 71, 69, and 48 kJ mol^{-1} for R = H, Me, Et, *i*-Pr, and *t*-Bu, respectively.[13] In a series of *N*,*N*-dialkylacetamides CH_3CONR_2, $\Delta G^{\ddagger}$ are 78, 74, and 68 kJ mol^{-1} for R = Me, Et, and *i*-Pr, respectively.[14]

In a series of *N*-alkyl-*N*-9-triptycylacetamides **2**—**4**, the $\Delta G^{\ddagger}$ values are in the order **4** (Bzl) > **2**(Me) ≫ **3** (Et) in any solvent examined (Table 6), Again the order is not parallel with the bulkiness of the alkyl group. The barriers for **2** and **4** are lower than those for CH_3CONMe_2 and CH_3CONEt_2 (vide supra) and that for **3** is even lower. This may partly be explained by the following reasoning. We now assume that the ground state geometry in solution is similar to that found in crystal. Along with the increase in pyramidality in the ground state, the double-bond character of the amide bond will decrease and this will result in the decrease in the barrier. If this factor is important, the barrier order of **3** > **2** > **4** would be expected judging from the observed order of pyramidality in crystal. The observed order of the barrier is just the reverse, and this suggests the contribution of other factors. The dihedral angle C7–N–C3–C4 (see Scheme 2 and Table 1) is smaller in **3** (23°) than in **2** or **4** (> 40°), and thus destabilization of the ground state due to the steric repulsion between the R and the *o*-benzeno groups will be greater in **3** than in **2** or **4**. If we assume that the steric bulk of R does not significantly affect the transition state energy, then the energy barrier in **3** is expected to be lower than those in **2** or **4**, which is actually found.

As for the solvent effects, the barrier ($\Delta G^{\ddagger}$) increases as the solvent is changed from nonpolar CCl_4 and toluene to polar $CDCl_3$, CD_2Cl_2, and acetone, then to the hydroxylic solvents, ethanol and methanol. These tendencies have generally been observed in amides and are ascribed to the more polar nature of the ground state than the transition state for rotation. The problem has recently been reinvestigated and discussed by Wiberg et al.[15] Although the nitrogen atom in **2**—**4** is somewhat pyramidalized, the degree of pyramidality should be far smaller than in the transition state. And thus a polar solvent will stabilize the ground state more effectively than the transition state, and a hydroxylic solvent will hydrogen-bond more strongly with the ground state than with the transition state. Figure 5 shows the plot of $\Delta G^{\ddagger}$ values for compound **4** against $\Delta G^{\ddagger}$ for *N*,*N*-dimethylacetamide[15] in several solvents, and this indicates that the solvent effect on these compounds is almost parallel.

The $\Delta S^{\ddagger}$ values tend to be more negative as the solvent becomes more polar, but we refrain from further discussion based on the $\Delta H^{\ddagger}$ and $\Delta S^{\ddagger}$ values because the data contain large errors and the solvent dependence is too complex to be interpreted in a simple way.

Stereodynamics about the Tp–N Bond. Changes in the ^{1}H NMR lineshape due to the stereomutation around the Tp–N bond are observed below ambient temperature, although the spectra are sometimes complicated by the lineshape changes due to the $E \rightleftarrows Z$ isomerization of the amide bond. Some details are described below for each compound examined.

In compound **1** which exists solely as the *Z*-isomer, three

Table 6. Kinetic Parameters for the $Z \rightleftarrows E$ Interconversion in Compounds **2**—**4** in Various Solvents[a)]

Solvent		**2**			**3**			**4**		
		$\Delta H^{\ddagger}$	$\Delta S^{\ddagger}$	$\Delta G^{\ddagger}_{300K}$	$\Delta H^{\ddagger}$	$\Delta S^{\ddagger}$	$\Delta G^{\ddagger}_{300K}$	$\Delta H^{\ddagger}$	$\Delta S^{\ddagger}$	$\Delta G^{\ddagger}_{300K}$
CCl_4	$Z \rightarrow E$	69.2±2.3	11.8±7.6	65.6				72.1±2.8	18.2±9.4	66.6
	$E \rightarrow Z$	67.6±2.2	12.6±7.1	63.8				69.8±2.8	14.7±9.4	65.4
$C_6D_5CD_3$	$Z \rightarrow E$	65.9±2.1	−1.8±7.2	66.4	56.1±1.9	−5.4±6.8	57.7	70.7±1.6	12.8±5.1	66.8
	$E \rightarrow Z$	60.9±2.3	−7.9±7.7	63.3	56.7±2.3	−11.0±8.2	60.0	67.1±1.6	6.3±5.1	65.2
$CDCl_3$	$Z \rightarrow E$	75.7±2.1	19.9±6.7	69.7	67.0±1.2	18.2±4.0	61.5	78.1±4.7	26±15	70.4
	$E \rightarrow Z$	69.9±1.9	11.5±6.0	66.4	62.9±1.1	−0.6±3.9	63.1	73.3±4.9	17±16	68.1
CD_2Cl_2	$Z \rightarrow E$	b)			67.6±1.7	13.6±6.3	63.5	71.1±7.8	−3±27	72.0
	$E \rightarrow Z$				60.0±1.6	−5.6±5.6	61.6	63.9±7.7	−13±26	67.8
$(CD_3)_2CO$	$Z \rightarrow E$	b)			61.9±3.7	2±13	61.3	63.0±7.1	−26±25	70.7
	$E \rightarrow Z$				56.1±3.9	−12±14	59.6	55.3±7.1	−36±25	66.0
C_2D_5OD	$Z \rightarrow E$	65.8±6.3	−21±21	72.0	60.7±4.0	−11±14	63.9	64.6±7.6	−25±25	72.2
	$E \rightarrow Z$	56.3±6.4	−36±22	67.1	57.9±4.1	−21±14	64.1	57.2±7.6	−38±25	68.6
CD_3OD	$Z \rightarrow E$	b)			62.2±2.1	−10.7±7.5	65.5	72±11	−7±35	73.8
	$E \rightarrow Z$				58.1±2.3	−20.3±8.0	64.2	63±11	−22±36	69.4

a) $\Delta H^{\ddagger}$ and $\Delta G^{\ddagger}_{300K}$ are given in kJ mol^{-1} and $\Delta S^{\ddagger}$ in J mol^{-1} K^{-1}. b) Not measured because the isomer equilibrium is too one-sided.

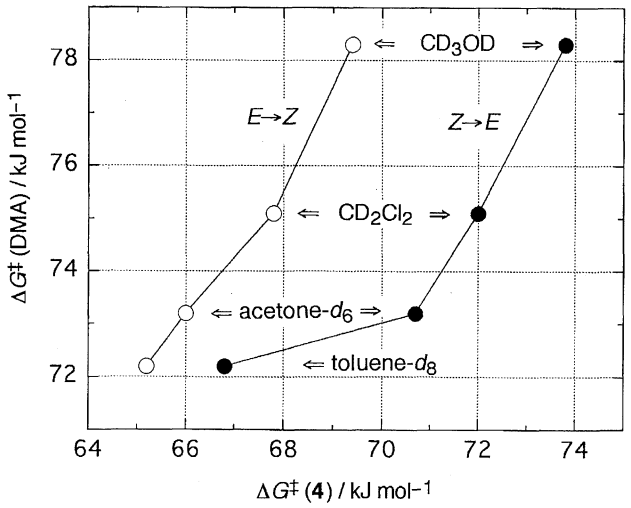

Fig. 5. The plot of $\Delta G^{\ddagger}$ for *N*,*N*-dimethylformamide and $\Delta G^{\ddagger}$ for compound **4** in several solvents.

o-benzeno groups are magnetically equivalent at ambient temperature, as typically shown by the appearance of only six peaks for the aromatic carbons. Two quaternary carbon signals are observed at δ = 142.9 and 144.6 in CD_2Cl_2. Upon lowering the temperature, the aromatic carbon signals broaden and split, reflecting the slowing-down of the stereomutation, or more strictly, the passing of the acetyl group over an *o*-benzeno group (this process is hereafter referred to as "Ac-passing"). At −100 °C, the aromatic quaternary carbons appear as two pairs of peaks in a ratio of 2 : 1, two large peaks at δ = 141.8 and 143.2 and two small peaks at δ = 142.8 and 145.6, indicating that one of the *o*-benzeno groups is magnetically different from the other two. This is interpreted so that the Ac-passing is frozen. Here we infer that the nitrogen is planar as shown in crystal, or that the nitrogen inversion is fast on the NMR time scale even if the nitrogen is pyramidal. The corresponding spectral changes with temperature are also observed in the ^{1}H NMR spectrum of **1**. The aromatic proton signals at various temperatures are shown in Fig. 6. The signals ascribed to the *peri*-protons (1-, 8-, and 13-H) are observed at δ = 7.3 at 25 °C, which decoalesces into 2 : 1 signals that appear at δ = 7.25 and 7.45 at −91 °C. Although no quantitative lineshape analysis has been made, the rate constant for the Ac-passing is roughly estimated to be ca. 100 s^{-1} at ca. −70 °C from the coalescence of the *peri*-proton signals, which gives $\Delta G^{\ddagger}$ of ca. 40 kJ mol^{-1} at this temperature.

Compound **2** exists in CD_2Cl_2 almost as the *Z*-isomer especially at low temperature as mentioned above (Table 4), and thus only the dynamic behavior of the (*Z*)-**2** is deduced from the spectral change. The observed change is quite similar as that for **1**. The three *o*-benzeno groups of the Tp moiety are equivalent at ambient temperature, but at −100 °C one *o*-benzeno group is nonequivalent from the other two.

It would be reasonable to assume that *N*-alkyl-*N*-9-triptycylacetamides **2**—**4** adopt chiral conformations similar to those observed in crystal, which are schematically shown in Newman-type projections in Scheme 3. The acetyl group

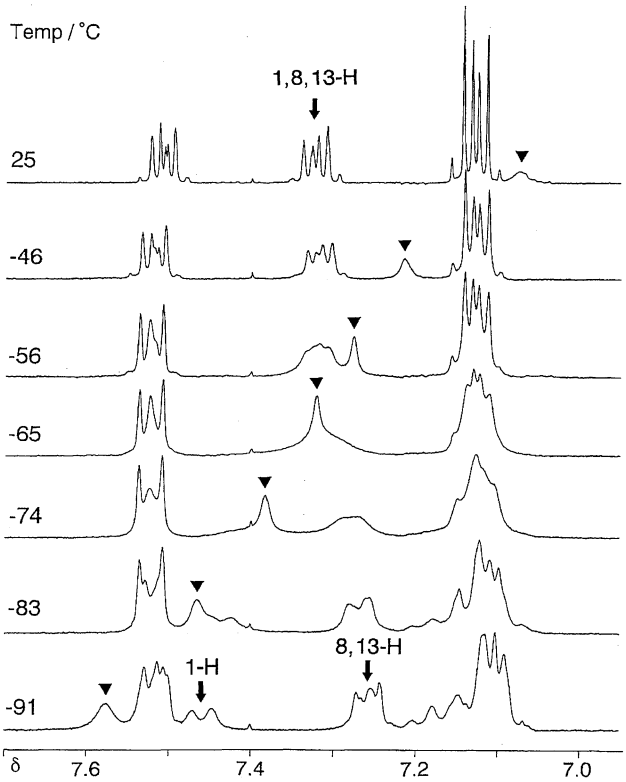

Fig. 6. The aromatic proton region spectra of compound **1** in CD_2Cl_2 at various temperatures. Signals with ▼ are due to NH.

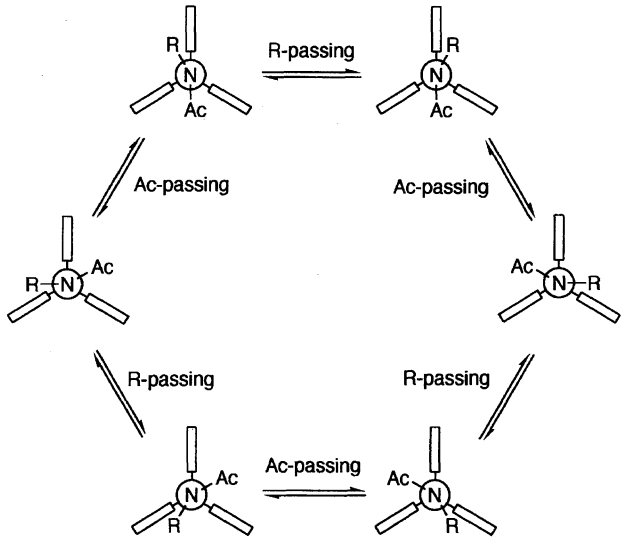

Scheme 3.

(Ac) and an alkyl group (R) occupy two different notches made by two *o*-benzeno groups. In order to interconvert these conformations, two types of rate processes are considered: "Ac-passing" and "R-passing", where the Ac or R group passes over one of the *o*-benzeno groups (Scheme 3). Either process involves nitrogen inversion and converts a conformation to its enantiomer.[16] When both processes are fast on the NMR time scale, three *o*-benzeno groups are equivalent. Meanwhile, when both processes are slow, three *o*-benzeno groups are mutually nonequivalent. In the case

where one of the processes is slow and the other is fast, two of the *o*-benzeno groups are equivalent but the third is different from the other two.

The situation of compound **2** at −100 °C corresponds to the third case. It is reasonably assumed that "Ac-passing" has a higher barrier than "R-passing" (Me-passing in this case) judging from the relative steric bulkiness of the Ac and Me groups. It is thus inferred that Ac-passing is frozen but Me-passing is still fast at −100 °C. Broadening and coalescence of the aromatic signals are observed with the increase of the temperature, reflecting the acceleration of Ac-passing. $\Delta G^{\ddagger}$ for Ac-passing is roughly estimated to be ca. 40 kJ mol^{-1} at ca. −70 °C, while that for Me-passing is far below 35 kJ mol^{-1}.

In compounds **3** and **4**, both of *Z*- and *E*-isomers are present in comparable amounts in any solvent, and the spectral changes with temperature are significantly complex. As typical examples, the methylene and aromatic signals of **4** in toluene-d_8 at several temperatures are shown in Figs. 7 and 8. At −70 °C, the methylene protons give a pair of doublets for each isomer: larger doublets at δ = 4.43 and 4.90 (J = 19.2 Hz) for (*Z*)-**4** and smaller ones at δ = 4.67 and 5.55 (J = 17.3 Hz) for (*E*)-**4** (Fig. 7). This feature corresponds to the situation where both Ac-passing and R-passing are frozen on the

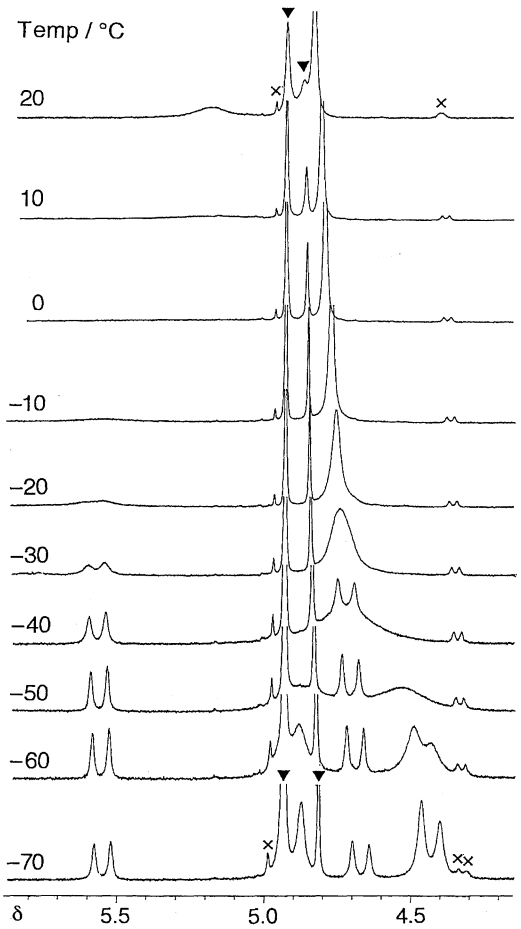

Fig. 7. The methylene proton region spectra of compound **4** in toluene-d_8 at various temperatures. Signals with ▼ are due to 10-H and those with × are due to impurities.

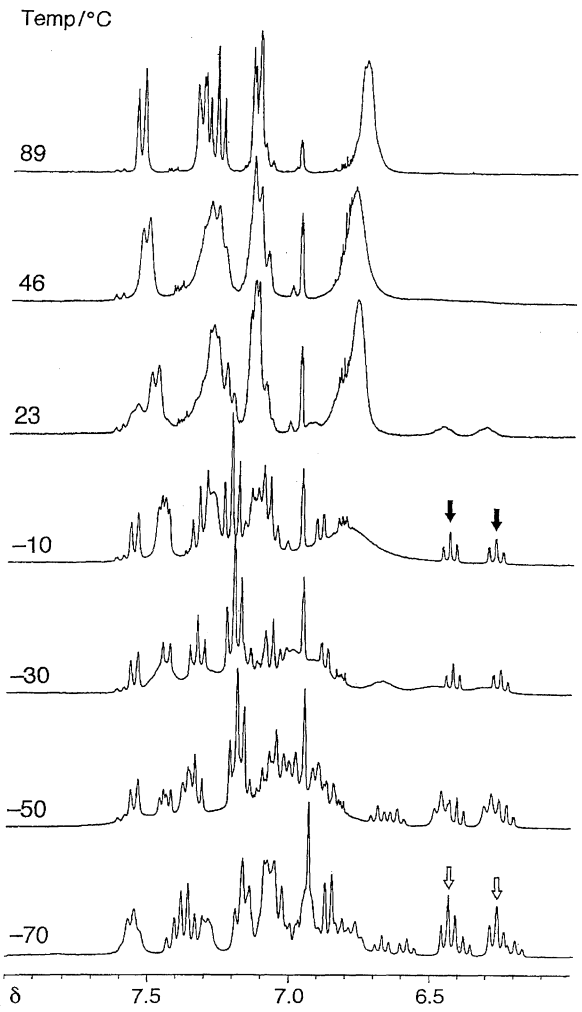

Fig. 8. The aromatic proton region spectra of compound **4** in toluene-d_8 at various temperatures. For signals with arrows, see text.

NMR time scale. And this strongly suggests that the nitrogen atom is pyramidalized also in solution. The aromatic proton spectrum at −70 °C is too complex to analyze (Fig. 8).

Upon raising the temperature, the methylene signal for (*Z*)-**4** coalesces into a single peak at ca. −45 °C, while that for (*E*)-**4** coalesces at ca. 0 °C (Fig. 7). Either Ac-passing or R-passing (Bzl-passing in this case) causes the coalescence of the methylene signal and therefore the rate constant obtained from the lineshape analysis is a sum of rate constants for these two processes ($k_{obs} = k_{Bzl} + k_{Ac}$). The relative contribution of the two processes can not be determined from the analysis of the methylene signal, but additional information is obtained from the behavior of the aromatic proton signals shown in Fig. 8. At −10 °C, two triplets are observed at the highest-field region (marked with ↓). These signals are unambiguously assigned to 2-H and 3-H (on the *o*-benzeno ring located near the benzyl group; see Scheme 4) of the *E*-isomer judging from the relative intensities, chemical shifts, and multiplicities. The fact that the signals for 2-H and 3-H of (*E*)-**4** are sharp at −10 °C and are before coalescence even at 23 °C (Fig. 8), together with the fact that the methylene

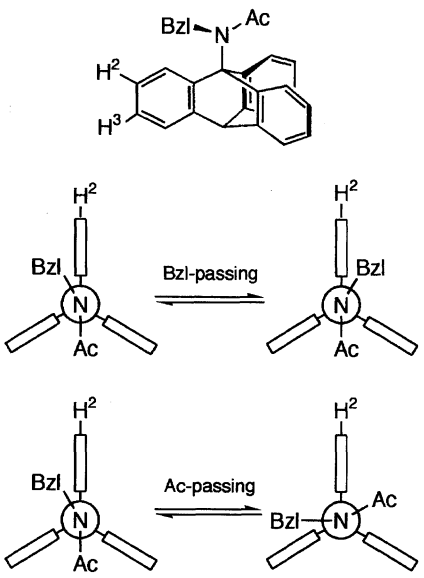

Scheme 4.

proton signal of (*E*)-**4** almost coalesces at −10 °C (Fig. 7), clearly indicates that Bzl-passing is significantly faster than Ac-passing ($k_{Bzl} \gg k_{Ac}$), because Bzl-passing does not affect the lineshape of the 2-H or 3-H signal but Ac-passing induces the coalescence of the signal (Scheme 4). The same argument can be made for (*Z*)-**4** from the behavior of the signals assigned to 2-H and 3-H of (*Z*)-**4** (marked with ⇓ in Fig. 8). The Bzl-passing process is therefore concluded to be faster than Ac-passing in both isomers of **4**.

Rate constants are estimated to be ca. 600 s^{-1} at ca. 0 °C for (*E*)-**4** and ca. 330 s^{-1} at −45 °C for (*Z*)-**4** from the methylene signals using the coalescence approximation, which correspond to $\Delta G^{\ddagger}$ of 52 and 44 kJ mol^{-1} for (*E*)-**4** and (*Z*)-**4**, respectively. As discussed above, these parameters are approximated to be those for Bzl-passing (i.e. $k_{obs} \approx k_{Bzl}$). The higher barrier to Bzl-passing in (*E*)-**4** than in (*Z*)-**4** may be explained as follows. The carbonyl oxygen opposes to the Tp moiety in (*Z*)-**4**, while the methyl group directly interacts with the Tp moiety in (*E*)-**4**. Thus the transition state for Bzl-passing in (*E*)-**4** may be more destabilized than that in (*Z*)-**4** due to the more severe buttressing effect, resulting in the higher barrier in (*E*)-**4**,

Lineshape changes reflecting the occurrence of Ac-passing should appear in the aromatic region spectrum in both ^{1}H and ^{13}C NMR at a higher temperature range than those due to Bzl-passing. Analysis of the ^{1}H spectrum seems difficult as typically shown in Fig. 8. Furthermore, the concomitant occurrence of the $E \rightleftarrows Z$ isomerization makes the analysis even more difficult. Thus quantitative analysis of Ac-passing has so far been abandoned.

As for the *N*-ethyl compound **3**, similar spectral changes with temperature as those found for **4** are observed, though at lower temperatures than in the case of **4**. Figure 9 shows the temperature dependence of the methylene signal of **3** in toluene-d_8. At 30 °C, the methylene protons give a broad signal because of fast stereomutation about the amide and Tp–N bonds. Upon lowering the temperature, the signal

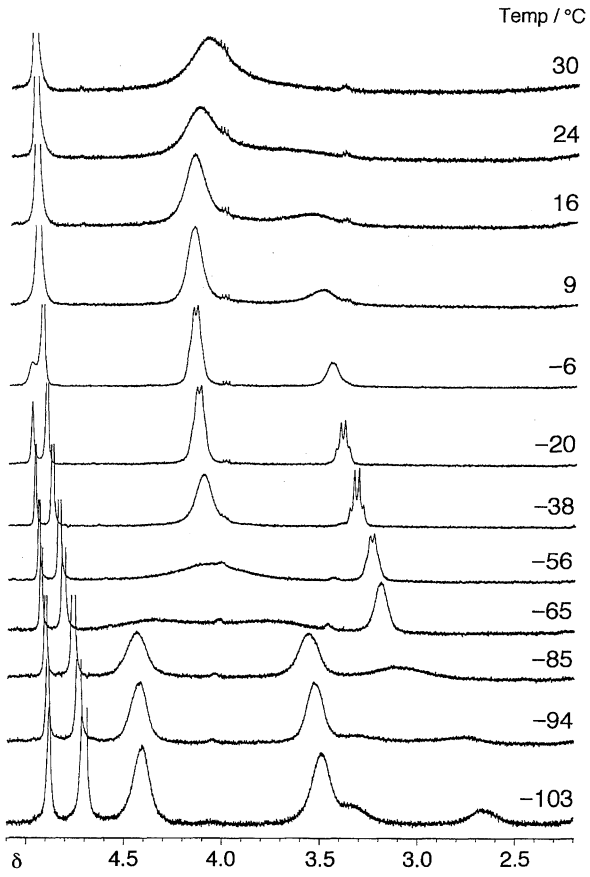

Fig. 9. The methylene proton region spectra of compound **3** in toluene-d_8 at various temperatures. Signals at the lowest field are due to 10-H.

splits into two due to the slow-down of the amide bond rotation, the higher-field signal being ascribed to (*Z*)-**3**. The $E \rightleftarrows Z$ process is almost frozen around −20 °C, where the methylene protons are mutually equivalent in either isomer. Further lowering of the temperature causes the splitting of both signals into two for each because of the slow-down of both Ac-passing and R-passing (Et-passing in this case), although the processes are not completely frozen even at −103 °C. The aromatic proton region spectrum shows a complex overlap of signals, but at −20 °C a sharp doublet signal corresponding to one proton of (*E*)-**3** is observed at the lowest field separated from the other signals, indicating that one of the *o*-benzeno group is nonequivalent from the other two. The signal is tentatively assigned to 1-H (on the *o*-benzeno ring near the ethyl group), but the assignment does not matter in the following discussion. Broadening of this signal occurs above 0 °C, while the coalescence of the methylene signal of (*E*)-**3** occurs at ca. −60 °C as shown in Fig. 9. This clearly indicates that either one of Ac-passing and Et-passing is slow and the other is fast on the NMR timescale at −20 °C. Judging from the discussion above for **4** and the smaller size of ethyl than benzyl, it will be reasonably argued that Et-passing is far faster than Ac-passing in (*E*)-**3**.

As for (*Z*)-**3**, coalescence of the methylene signal at ca. −90 °C (Fig. 9) and appearance of a unique one proton signal at the lowest-field of the aromatic region below −70

Table 7. $\Delta G^{\ddagger}$ (kJ mol^{-1}) for the Processes in Stereomutation around the Tp–N Bond[a)]

Compd	Solvent	Isomer	Ac-passing	R-Passing
1	CD_2Cl_2	*Z*	40 (−70)	—
2	CD_2Cl_2	*Z*	40 (−70)	≪ 35 (< −100)
3	$C_6D_5CD_3$	*Z*		35 (−70)
		E		40 (−60)
4	$C_6D_5CD_3$	*Z*		44 (−45)
		E		52 (0)

a) Reliable to ±2 kJ mol^{-1}. In parenthese are the "coalesence" temperatures in °C (±10 °C).

°C suggest that one of the two processes is fast and the other slow in the −70—−90 °C range. Again Et-passing is argued to have a lower barrier than Ac-passing in (*Z*)-**3**. Analysis of the lineshape change in the methylene proton signals by the coalescence approximation affords rate constants for Et-passing as ca. 500 s^{-1} at ca. −60 °C for (*E*)-**3** and ca. 400 s^{-1} at ca. −90 °C for (*Z*)-**3**, which correspond to $\Delta G^{\ddagger}$ of ca. 40 and ca. 35 kJ mol^{-1}, respectively.

The $\Delta G^{\ddagger}$ values for the processes in the stereomutation around the Tp–N bond are compiled in Table 7. The R-passing barrier increases with the bulkiness of R, and is higher for the *E*-isomer than for the *Z*-isomer, as discussed earlier. The Ac-passing barrier also seems to increase with R, although no quantitative values for the barrier height are available.

The stereochemical behavior of *N*-9-triptycylacetamides carrying a primary alkyl group at the nitrogen have been reported in this paper, and studies on those with a secondary alkyl or an aryl group are now in progress.

Experimental

General. Melting points are not corrected. ^{1}H and ^{13}C NMR spectra were obtained on a Bruker ARX-300 spectrometer operating at 300.1 MHz for ^{1}H and 75.4 MHz for ^{13}C, respectively. Chemical shifts were referenced with internal tetramethylsilane (δ_H = 0) or $CDCl_3$ (δ_C = 77.0). Data of ^{1}H and ^{13}C spectra given below are those obtained at 22—24 °C. Letters p, s, t, and q given with the ^{13}C chemical shifts denote primary, secondary, tertiary, and quaternary, respectively. In variable-temperature experiments, temperatures were calibrated using a methanol or an ethylene glycol sample and are reliable to ±1 °C.

***N*-9-Triptycylacetamide (1).** A solution of 269 mg (1.0 mmol) of 9-triptycylamine (**5**)[6b,17] in 5.0 mL of acetic anhydride was heated under reflux for 1.5 h. After being cooled to room temperature, the reaction mixture was poured into 100 mL of water and digested. The precipitates formed were collected by filtration, washed with water, and dried, affording 292 mg (94%) of **1**. Recrystallization from dichloromethane–hexane gave a pure sample of **1** as colorless crystals, mp 323—325 °C. Found: C, 84.88; H, 5.66; N, 4.54%. Calcd for $C_{22}H_{17}NO$: C, 84.86; H, 5.50; N, 4.50%. IR (KBr) 3330, 1658 cm^{-1}. ^{1}H NMR ($CDCl_3$) δ = 2.52 (3H, s, CH_3), 5.40 (1H, s, 10-H), 6.98 (1H, br s, NH), 6.98—7.06 (6H, m), 7.24 (3H, m), 7.40 (3H, m). ^{13}C NMR ($CDCl_3$) δ = 24.43 (1C, p, CH_3), 53.60 (1C, t, 10-C), 66.59 (1C, q, 9-C), 120.89 (3C, t), 123.67 (3C, t), 124.73 (3C, t), 125.63 (3C, t), 142.39 (3C, q), 144.16 (3C, q), 169.72 (1C, q, C=O).

***N*-Methyl-9-triptycylamine (6).** To a stirred mixture of 2.16 g (8.02 mmol) of 9-triptycylamine (**5**) and 1.33 g (9.62 mmol) of potassium carbonate in 50 mL of dry THF was added dropwise 0.6 mL (9.64 mmol) of methyl iodide and the mixture was heated under reflux for 12 h. After filtration of the solid mass, the solution was evaporated and the residue was chromatographed through alumina with hexane–dichloromethane as the eluent to give 0.65 g (26%) of **6**, mp 197—199 °C (lit,[6b] 199–200 °C), together with similar amounts of *N*,*N*-dimethyl-9-triptycylamine and **5**.[6b]

***N*-Methyl-*N*-9-triptycylacetamide (2).** To a solution of 187 mg (0.66 mmol) of *N*-methyl-9-triptycylamine (**6**) in 40 mL of dichloromethane was added 1.0 mL (14 mmol) of acetyl chloride and the mixture was stirred for 3 h at ambient temperature. The white precipitates which formed were filtered off and the filtrate was washed successively with water, aq $NaHCO_3$, and brine, and dried over $MgSO_4$. After removal of the solvent, the residue was sublimed at reduced pressure to give 79 mg (37%) of **2**, mp 190—191 °C. Found: C, 84.85; H, 5.96; N, 4.13%. Calcd for $C_{23}H_{19}NO$: C, 84.89; H, 5.89; N, 4.30%. IR (KBr) 1668, 1650 cm^{-1}. ^{1}H NMR ($CDCl_3$) *Z*-isomer: δ = 2.59 (3H, s), 3.70 (3H, s), 5.30 (1H, s); *E*-isomer: δ = 1.72 (3H, s), 3.85 (3H, s), 5.34 (1H, s); aromatic protons: δ = 6.8—7.8 (m); *Z*/*E* = 4.0. ^{13}C NMR ($CDCl_3$) δ = 174.5 (Z) and 178.0 (*E*).

***N*-Ethyl-9-triptycylamine (7).** (a) To a solution of 525 mg (1.68 mmol) of **1** in 30 mL of dry THF was added 9.7 mL (7.5 mmol) of BH_3·THF in THF (0.78 mol dm^{-3}) and the solution was heated under reflux for 45 h. After the reaction mixture was cooled to room temperature, diethyl ether (20 mL) was added, and the solution was washed successively with water and brine, and dried over $MgSO_4$. After evaporation of the solvent, the residue was recrystallized from CH_2Cl_2–hexane to afford 248 mg (49%) of **7**, mp 189—190 °C (lit,[6b] 191—192 °C).

(b) To a solution of 532 mg (1.71 mmol) of **1** in 50 mL of dry THF was added 390 g (10.3 mmol) of $LiAlH_4$ and the mixture was heated under reflux for 3 d. After quenching the excess reagent with ethyl acetate and water, the mixture was extracted with dichloromethane. The organic layer was washed with water, dried over $MgSO_4$ and concentrated. Preparative TLC of the residue afforded 183 mg (36%) of **7**.

***N*-Ethyl-*N*-9-triptycylacetamide (3).** To a solution of 183 mg (0.62 mmol) of **7** in 10 mL of dichloromethane was added 1.0 mL (14 mmol) of acetyl chloride and the mixture was stirred for 3 h at ambient temperature. The white precipitates which formed were filtered off and the filtrate was washed successively with water, aq $NaHCO_3$, and brine, and dried over $MgSO_4$. After removal of the solvent, the residue was recrystallized from ethanol to give 75 mg (36%) of **3**, mp 221—222 °C (lit,[6b] 221—222 °C).

***N*-9-Triptycylbenzamide (9).** A solution of 2.70 g (10 mmol) of 9-triptycylamine (**5**), 2.32 g (20 mmol) of benzoyl chloride, and 3.5 mL (25 mmol) of triethylamine in 150 mL of dichloromethane was heated under reflux for 65 h. The solution was washed successively with water, aq $NaHCO_3$ and brine, and dried over $MgSO_4$. Recrystallization from hexane–dichloromethane afforded 3.22 g (86%) of **9**, mp 289 °C. Found: C, 86.84; H, 5.22; N, 3.72%. Calcd for $C_{27}H_{19}NO$: C, 86.84; H, 5.13; N, 3.75%. ^{1}H NMR ($CDCl_3$) δ = 5.447 (1H, s, 10-H), 7.00—7.07 (6H, m), 7.28—7.36 (3H, m), 7.38—7.46 (3H, m), 7.57—7.70 (4H, m, *m*- and *p*-H, NH), 8.17—8.23 (2H, m, *o*-H). ^{13}C NMR ($CDCl_3$) δ = 53.66 (1C, t, 10-C), 66.73 (1C, q, 9-C), 120.95 (3C, t), 123.70 (3C, t), 124.82 (3C, t), 125.68 (3C, t), 127.36 (2C, t), 129.07 (2C, t), 132.18 (1C, t), 135.03 (1C, q), 142.50 (3C, q), 144.22 (3C, q), 167.05 (1C, q, C=O).

***N*-Benzyl-9-triptycylamine (8).** To a solution of 2.24 g (6.0

mmol) of *N*-9-triptycylbenzamide (**9**) in 90 mL of THF was added 30.8 mL (24 mmol) of BH_3·THF in THF (0.78 mol dm^{-3}) and the solution was heated under reflux for 110 h. After evaporation of most of the THF, the residue was partitioned with dichloromethane and water. The organic layer was washed with water and brine, dried over $MgSO_4$ and evaporated. The residue was recrystallized from dichloromethane–hexane to afford 1.81 g (84%) of **8**, mp 172—173 °C (lit,[6b] 180—181 °C).

***N*-Benzyl-*N*-9-triptycylacetamide (4).** To a solution of 1.80 g (5.0 mmol) of *N*-benzyl-9-triptycylamine (**8**) in 50 mL of dichloromethane was added 5.0 mL (70 mmol) of acetyl chloride, and the solution was heated under reflux for 18 h. After filtration of the formed salt, the filtrate was washed successively with water, aq $NaHCO_3$, and brine and dried over $MgSO_4$. After evaporation of the solvent, the residue was recrystallized from dichloromethane–hexane affording 0.37 g (18.5%) of **4**, mp 250.3—250.4 °C. The reaction in the presence of pyridine or triethylamine as the HCl-trap caused formation of a tarry mass and the desired product could not be isolated. Found: C, 86.83; H, 5.83; N, 3.46%. Calcd for $C_{29}H_{23}NO$: C, 86.75; H, 5.77; N, 3.48%. ^{1}H NMR ($CDCl_3$) *Z*-isomer: δ = 2.37 (3H, s), 5.32 (1H, s), 5.41 (2H, s); *E*-isomer: δ = 1.72 (3H, s), 5.36 (1H, s), ca. 5.43 (2H, br s); aromatic protons: δ = 6.60—7.74 (m).

Heating compound **8** under reflux in acetic anhydride for 5 h gave no detectable amount of **4**.

NMR Lineshape Analysis. Total lineshape analysis was performed by visual matching of experimental spectra with theoretical spectra computed on an NEC PC9821Xs personal computer equipped with a Mutoh PP-210 plotter using the DNMR3K program, a modified version of the DNMR3 program[18] converted for use on personal computers by Dr. H. Kihara of Hyogo University of Teacher Education. Temperature dependences of isomer populations, chemical shift differences and T_2 values were properly taken into account.

Saturation Transfer Experiments.[19] The proton signal due to the acetyl–methyl group of the *E*-isomer appearing at a higher field was irradiated and the change in the intensity of the lower-field acetyl–methyl signal due to the *Z*-isomer was observed. Nonlinear least-squares analysis of the data afforded rate constants for the $Z \rightarrow E$ process.

Molecular Mechanics Studies. Molecular mechanics calculations were performed employing the MM3 program[20] with the 1989 force field on an NEC EWS-4800/360 work station. These torsional and bending parameters were added: 2-1-9-1: V_3 = 0.91; 2-1-9-3: V_1 = −0.3, V_3 = 0.3; 9-1-2-2: V_1 = 0.25, V_2 = −0.65, V_3 = 0.6; 2-1-9: k_s = 0.43, θ_0 = 110.0. These values were chosen consulting the existing parameters in the force field, but some of them might be inadequate and cause the discrepancies mentioned in the text.

X-Ray Crystallography. Crystals of compounds **1**, **2**, and **4** were grown from dichloromethane–hexane, while those of **3** were from ethanol and contained one-half equivalent of water. Crystals of **3** grown from toluene gave the same crystal data as those from ethanol. The crystal data and the parameters for data collection, structure determination and refinement are summarized in Table 8. Diffraction data were collected on a Rigaku AFC7R diffractometer and calculations were performed using the SHELXL93 program.[21] The structure was solved by direct methods followed by full-matrix least-squares refinement with all non-hydrogen atoms anisotropic and hydrogen atoms isotropic. Reflection data with $|I| > 2\sigma(I)$ were used. The function minimized was $\sum w(|F_o| - |F_c|)^2$ where $w = [\sigma^2(F_o)]^{-1}$.

Table 8. Crystal Data of Compounds **1**—**4** and Parameters for Data Collection, Structure Determination, and Refinement

Compound	**1**	**2**	**3**	**4**
Empirical formula	$C_{22}H_{17}NO$	$(C_{23}H_{19}NO)_2$·H_2O	$C_{24}H_{21}NO$	$C_{29}H_{23}NO$
Formula weight	311.39	668.84	339.44	401.51
Crystal system	Monoclinic	Monoclinic	Triclinic	Monoclinic
Space group	$P2_1/n$	$P2_1/n$	$P\bar{1}$	$P2_1/c$
a/Å	8.334(6)	9.707(1)	12.399(2)	11.521(3)
b/Å	23.987(11)	27.159(8)	15.481(2)	8.159(6)
c/Å	9.178(5)	13.552(2)	9.502(2)	22.954(3)
α/°	90.00	90.00	103.58(1)	90.00
β/°	113.86(5)	99.92(1)	99.66(2)	95.70(2)
γ/°	90.00	90.00	90.06(2)	90.00
V/Å^3	1678.0(17)	3519.5(11)	1746.2(6)	2146.9(16)
Z	4	4	4	4
D_c/g cm^{-3}	1.233	1.262	1.291	1.242
F(000)	656	1416	720	848
μ(Mo $K\alpha$)/cm^{-1}	0.075	0.078	0.078	0.075
Temp/°C	25±2	20±2	20±2	20±2
Scan width/°	1.103±0.30 tan θ	0.735±0.30 tan θ	1.313±0.30 tan θ	1.313±0.30 tan θ
$2\theta_{max}$/°	60.0	55.0	55.0	55.0
No. of reflections measured				
Total	4897	8103	8024	4938
Unique	3101	4787	6129	1694
No. of refinement variables	285	616	637	372
Final R ; R_w	0.0546; 0.1364	0.0553; 0.1413	0.0492; 0.1354	0.0562; 0.1039

$R = \sum||F_o| - |F_c||/\sum|F_o|$, R_w on F^2.

References

1 W. E. Stewart and T. H. Siddall, III, *Chem. Rev.*, **70**, 517 (1970); M. Ōki, "Applications of Dynamic NMR Spectroscopy to Organic Chemistry," VCH, New York (1985), Chap. 2; M. Pinto, in "Acyclic Organonitrogen Stereodynamics," ed by J. B. Lambert and Y. Takeuchi, VCH, New York (1992), Chap. 5.

2 See for example: K. B. Wiberg and K. E. Laidig, *J. Am. Chem. Soc.*, **109**, 5935 (1987); K. B. Wiberg and C. M. Breneman, *J. Am. Chem. Soc.*, **114**, 831 (1992); A. Greenberg, D. T. Moore, and T. D. DuBois, *J. Am. Chem. Soc.*, **118**, 8658 (1996).

3 See for example: T. G. Lease and K. J. Shea, *J. Am. Chem. Soc.*, **115**, 2248 (1993); A. Greenberg and C. A. Venanzi, *J. Am. Chem. Soc.*, **115**, 6951 (1993); A. Greenberg, D. T. Moore, and T. D. Dubois, *J. Am. Chem. Soc.*, **118**, 8658 (1996); A. J. Kirby, I. V. Komarov, P. D. Wothers, and N. Feeder, *Angew. Chem., Int. Ed. Engl.*, **37**, 785 (1998).

4 S. Yamada, *Angew. Chem., Int. Ed. Engl.*, **32**, 1083 (1993); S. Yamada, *J. Org. Chem.*, **61**, 941 (1996), and references cited therein.

5 T. Ohwada, T. Achiwa, I. Okamoto, K. Shudo, and K. Yamaguchi, *Tetrahedron Lett.*, **39**, 865 (1998).

6 a) G. Yamamoto, H. Higuchi, M. Yonebayashi, and J. Ojima, *Chem. Lett.*, **1994**, 1911. b) G. Yamamoto, H. Higuchi, M. Yonebayashi, Y. Nabeta, and J. Ojima, *Tetrahedron*, **52**, 12409 (1996).

7 G. Yamamoto, H. Higuchi, M. Yonebayashi, Y. Nabeta, and J. Ojima, *Chem. Lett.*, **1995**, 853; G. Yamamoto, K. Inoue, H. Higuchi, M. Yonebayashi, Y. Nabeta, and J. Ojima, *Bull. Chem. Soc. Jpn.*, **71**, 1241 (1998).

8 G. Yamamoto, K. Kuwahara, and K. Inoue, *Chem. Lett.*, **1995**, 351.

9 Preliminary results have been reported: a) G. Yamamoto, H. Murakami, N. Tsubai, and Y. Mazaki, *Chem. Lett.*, **1997**, 605. b) G. Yamamoto, N. Tsubai, H. Murakami, and Y. Mazaki, *Chem. Lett.*, **1997**, 1295.

10 See for example: N. Nogami, M. Ōki, S. Sato, and Y. Saito, *Bull. Chem. Soc. Jpn.*, **55**, 3580 (1982).

11 J. V. Hatton and R. E. Richards, *Mol. Phys.*, **3**, 253 (1960); **5**, 139 (1962).

12 L. A. Laplanche and M. T. Rogers, *J. Am. Chem. Soc.*, **85**, 3728 (1963).

13 T. Drakenberg, K.-I. Dahlqvist, and S. Forsén, *J. Phys. Chem.*, **76**, 2178 (1972).

14 T. H. Siddall, III, W. E. Stewart, and F. D. Knight, *J. Phys. Chem.*, **74**, 3580 (1970).

15 K. B. Wiberg, P. R. Rablen, D. J. Rush, and T. A. Keith, *J. Am. Chem. Soc.*, **117**, 4261 (1995).

16 Rotation of the Tp–N bond without the nitrogen inversion is inferred to require a far higher energy than these processes, and thus not considered. If this process had the lowest barrier, the three *o*-benzeno groups should become equivalent faster than the methylene protons becoming equivalent in **3** and **4**, and that is not observed.

17 P. D. Bartlett and F. D. Greene, *J. Am. Chem. Soc.*, **76**, 1088 (1954); W. Theilacker and K.-H. Beyer, *Chem. Ber.*, **94**, 2968 (1961); H. Quast and B. Seiferling, *Liebigs Ann. Chem.*, **1982**, 1566.

18 D. A. Kleier and G. Binsch, "QCPE Program No. 165".

19 S. Forsén and R. A. Hofmann, *J. Chem. Phys.*, **39**, 2892 (1963); J. Sandström, "Dynamic NMR Spectroscopy," Academic Press, London (1982), Chap. 4; G. Yamamoto, *Bull. Chem. Soc. Jpn.*, **65**, 1967 (1992).

20 The program was obtained from the Technical Utilization Corporation.

21 G. M. Sheldrick, "Program for the Refinement of Crystal Structures." University of Göttingen, Germany (1993).